$A^3\Sigma^+_u$ molecules in the N_2 afterglow

D. E. Shemansky

*Department of Physics, University of Pittsburgh, Pittsburgh, Pennsylvania 15260**
(Received 20 August 1974; revised paper received 6 October 1975)

Excitation of N_2 by electrons with energy below the ionization threshold produces a strong afterglow in the $B^3\Pi_g$–$A^3\Sigma^+_u$ system. The precursor is identified as the $A^3\Sigma^+_u$ state in the $v>6$ vibrational levels. The peak electron cross section of the $A^3\Sigma^+_u$–$X^1\Sigma^+_g$ system is estimated at about three times the $B^3\Pi_g$–$X^1\Sigma^+_g$ transition. Deactivation rates of the $A^3\Sigma^+_u$ $v>6$ levels by $X^1\Sigma^+_g$ molecules vary over the $8E-12$ cm^3sec^{-1}–$5E-11$ cm^3sec^{-1} range. There is some evidence that the higher levels may relax at rates comparable to that of electronic deactivation. Deactivation of $B^3\Pi_g$ by $X^1\Sigma^+_g$ molecules has a strong dependence on the vibrational level of the $B^3\Pi_g$ state. The rate coefficients for this process vary between $1E$-11 cm^3sec^{-1} and $1E-10$ cm^3sec^{-1}, with no measureable contribution by vibrational relaxation. The results suggest that production rates of the $B^3\Pi_g$ state in the Lewis–Rayleigh (L–R) afterglow are much more uniformly distributed over the vibrational levels than has been previously assumed. We also suggest it is unlikely that significant amounts of energy pass through the $^5\Sigma^+_g$ state in the L–R afterglow. About 25% of the energy of atomic nitrogen recombination enters the $B^3\Pi_g$ state in the L–R afterglow, according to the present results. The factors controlling the $A^3\Sigma^+_u$ $v=0,1$ population in the L–R afterglow appear to be much less well defined than has been suggested in previous literature.

INTRODUCTION

Over the years, published work on the yellow Lewis–Rayleigh afterglow of nitrogen has resulted in considerable disagreement on the nature of the processes determining the observed emission characteristics.[1] Most of the blame for this appears to be shared by the catalytic effects of trace impurities, and by the fact that the photoemissive systems under most conditions are rate limited by the source function, atomic nitrogen recombination. The precursor or precursors to the emissions have never been observed in a direct manner. The determination of the linkage between recombination and observed radiation is potentially of some importance to atmospheric processes, apart from the more direct interest in the kinetics of active nitrogen.

In recent years significant progress has been made through the work of Bayes and Kistiakowsky,[2] Noxon,[3] Young and Sharpless,[4] Campbell and Thrush,[5] Becker *et al.*,[6] and De Monchy,[7] in the direction of determining consistent, repeatable relationships of the various emissions to the atomic nitrogen population. The rate coefficients for three body atomic nitrogen recombination, and the mode of wall recombination appear to be well established judging by good agreement among the various measurements of Refs. 4–8. It appears to be generally agreed that virtually all of the energy for the L–R afterglow is derived from atomic nitrogen recombination.

Molecules in the $B^3\Pi_g$ state are the dominant emitters and give rise to the yellow glow through transitions in the N_2 first positive (1P) system. We accept as having been established that at pressures above 1 Torr and probably above 500 mTorr, the N_2 1P volume emission rate in pure N_2 is directly proportional to the square of atomic nitrogen density and independent of pressure.[4,5,9] However, the combination of two ground state N(4S) atoms does not correspond to the $B^3\Pi_g$ state[10] and we therefore require a precursor to the production of N_2 1P emission. The possibilities for recombination of N(4S) under ordinary circumstances reduce to the $^5\Sigma^+_g$, $A^3\Sigma^+_u$, and $X^1\Sigma^+_g$ states. A good summary of the proposed excitation modes and the effects of temperature, based on these possibilities can be found in the Anketell and Nicholls[11] review article. The major difficulty in providing an explanation through any of the precursor species alone or in combination has always been one of providing production mechanisms for the lower levels of the $B^3\Pi_g$ state, notably levels in the regions of $v=0$ and $v=6$. The most significant single factor in this context was first recognized by Campbell and Thrush[5]; the rate coefficients for deactivation of the $B^3\Pi_g$ state by N_2X are significantly large[12] such that the N_2 1P emission rate at pressures ≥ 1 Torr could only be a small fraction of the $B^3\Pi_g$ production rate. The implications of this were twofold. (1) The homogeneous recombination process for production of the precursor must be by three body recombination, and (2) a large fraction of the energy of recombination must be delivered through the $B^3\Pi_g$ state. Campbell and Thrush[5] presented an argument for production of all $B^3\Pi_g$ levels by atomic nitrogen recombination into the $A^3\Sigma^+_u$ state with subsequent vibrational relaxation and collision transfer into the $B^3\Pi_g$ state. Berkowitz *et al.*[13] and Bayes and Kistiakowsky[2] proposed processes involving the $^5\Sigma^+_g$ state and combinations of $^5\Sigma^+_g$ and $A^3\Sigma^+_u$ molecules, with intermediate reactions involving the $B^3\Sigma^-_u$ and $W^3\Delta_u$ states. The difficulty we encounter in attempting to distinguish the processes is rate limitation of $B^3\Pi_g$ production by the primary source under virtually all experimental conditions. The information thus cannot be obtained by direct means from observation of the L–R afterglow proper. Emission from $A^3\Sigma^+_u$ molecules is present in the afterglow, but from levels $v=0$, 1, that do not directly involve collision transfer into the $B^3\Pi_g$ state. Production and deactivation modes of the observed metastable levels are not obvious and the relationship to the higher $A^3\Sigma^+_u v>6$ levels is not at all clear. The situation is further complicated by the known energy pooling reaction of the $A^3\Sigma^+_u$ molecules, which can result in production of $C^3\Pi_u$, $B^3\Pi_g$, and $A^3\Sigma^+_u$ molecules.[13–15] A considerable amount of evidence for the deactivation of the $A^3\Sigma^+_u$ molecules by atomic nitrogen with a rate coefficient of $\sim 5\times10^{-11}$ cm^3sec^{-1} has appeared in the literature.[16–18] The observed $A^3\Sigma^+_u$–$X^1\Sigma^+_g$

emission shows a first order dependence on atomic nitrogen.[6,19] The high deactivation probability for N(4S) on $A\,^3\Sigma_u^+$ would then require that a large fraction of atomic nitrogen recombination must be ultimately deposited in the low $A\,^3\Sigma_u^+$ levels. However, an analysis by Shemansky[20] based in part on the new experimental measurements presented in this article, raises doubt as to whether a rate coefficient this large can be tolerated by the experimental evidence as a whole.

One factor that appears not to have been considered previously apart from a brief discussion by Shemansky and Broadfoot,[21a] is the question of how well the observed relative emission rates of the $B\,^3\Pi_g$ vibrational levels correspond to the production rates. The possibility of large variations in $B\,^3\Pi_g$ radiationless deactivation rates has been generally ignored. (However see Ref. 21b for estimates for $B\,^3\Pi_g\, v=0, 1$). The prospect of a significant alteration in the understanding of the afterglow processes because of this factor was in part the motivation for the experimental measurements described below.

The $B\,^3\Pi_g$ state excited in pure N_2 by electrons with energies below the ionization threshold displays a strong afterglow at pressures above 0.5 mTorr.[21] Atomic nitrogen recombination is ruled out as a source in this case due to the low energy of the exciting electrons. The Ref. 21 observations indicated high afterglow production rates in the $B\,^3\Pi_g\, v=6$, 10–12 levels, in rough correspondence with the L–R afterglow proper. It was concluded on the basis of magnitude and energy dependence of the purcursor electron cross section, that the source must be $A\,^3\Sigma_u^+ v>6$ molecules. The production of $A\,^3\Sigma_u^+$ molecules in this manner removes most of the complications that make observations of the L–R afterglow difficult to interpret. This article describes observations of the afterglow generated by low energy electrons in a static collision chamber. According to the present results the rate coefficients for deactivation of the $B\,^3\Pi_g$ state by $N_2 X$ vary between about 10^{-11} and 10^{-10} $cm^3 sec^{-1}$. The values are in rough agreement with the pulsed R–F discharge measurements of Ref. 12 commensurate with the fact that the latter experiment was not designed for estimating deactivation rates. There is spectacular disagreement with the low pressure L–R afterglow measurements of Ref. 6 with respect to the deactivation rates of the $B\,^3\Pi_g$ levels. The present results thus imply that the relative production rates of the $B\,^3\Pi_g$ levels in the L–R afterglow are distinctly different from the observed relative emission rates. The deactivation rates of the $A\,^3\Sigma_u^+ v>6$ levels by $N_2 X$ according the analysis given below vary between about 8×10^{-12} and 5×10^{-11} $cm^3 sec^{-1}$. No other comparable measurements are available in the literature. The observations do not contain sufficient information to determine what fraction of this rate results in $B\,^3\Pi_g$ production. However, all of the $B\,^3\Pi_g\, v<12$ levels display a strong second order afterglow in $[N_2]$, and the minimum peak $A\,^3\Sigma_u^+$ electron cross section calculated from steady state measurements is about 3×10^{-16} cm^2, a factor of 3 larger than the peak $B\,^3\Pi_g$ cross section. This minimum cross section is based on the assumption that all of the radiationless $A\,^3\Sigma_u^+$ state deactivation results in $B\,^3\Pi_g$ production. The observations suggest that $A\,^3\Sigma_u^+ v>6$ deactivation by $N_2 X$ may be mostly electronic and that very little vibrational relaxation occurs.

Following is a description of experimental measurements and discussion of the degenerate low pressure N_2 afterglow.

EXPERIMENTAL

A. General description

The gas is excited in a cylindrical stainless steel collision chamber with a 20 cm length and 30 cm diameter. An electrostatically focused electron gun used as the excitation source is contained in a small stainless steel housing with its own diffusion pump system. The electron gun housing is positioned in the collision chamber to allow an electron beam ~1.5 cm in length at the center of the chamber (Fig. 1). The chamber is evacuated with an ion pump system due to the importance of avoiding complications involving impurities which have produced inconsistant results in past experiments; atomic oxygen and hydrogen trace impurities are known to have a significant influence on the N_2 $B\,^3\Pi_g$ population distribution in the afterglow and NO is a strong deactivator of N_2 $A\,^3\Sigma_u^+$ molecules.

The observational instruments tied to the collision chamber are a refrigerated filter photometer and a vacuum spectrometer ($\frac{3}{4}$ m Czerny–Turner, Spex Industries). Data is obtained in the spectral region 1000–10 600 Å using pulse counting techniques. The detector used for most of the observations was an RCA C31034A photomultiplier tube cooled either by solid CO_2 or refrigeration. Observations longward of 8900 Å were obtained with the use of an ITT F4027 tube with S-1 type response.

The electron gun is electrostatically focused and designed for low energy operation. The cathode is a standard "oxide" type, indirectly heated. The electron beam is estimated to have an approximate 0.5 eV halfwidth at ~10 eV and current of ~5 μA as measured at the collector. Proper focusing of the beam required shielding of the chamber with "conetic" sheet. Transient excitation was accomplished by pulsing one of the focusing electrodes with a floating ~5 V monostable circuit, gated by computer program. The 90% rise–fall times of the gated beam were less than 10 nsec. The electron beam current was estimated to decrease 7 orders of magnitude with the application of the off cycle of the gating system, giving an output signal that was generally not distinguishable from dark noise of the photomultiplier tube (~0.5 count/sec).

Chamber pressure was measured and controlled through the use of an MKS Baratron capacitance monometer. Pressure was maintained within specified tolerances with a servo system connected to an on-line computer interrupt facility.

A Hewlett Packard 2116c computer is used to accumulate and analyze data, and to control the measurement system. Data was gathered through a programmable 50 Mhz counter–timer–digital voltmeter. The experi-

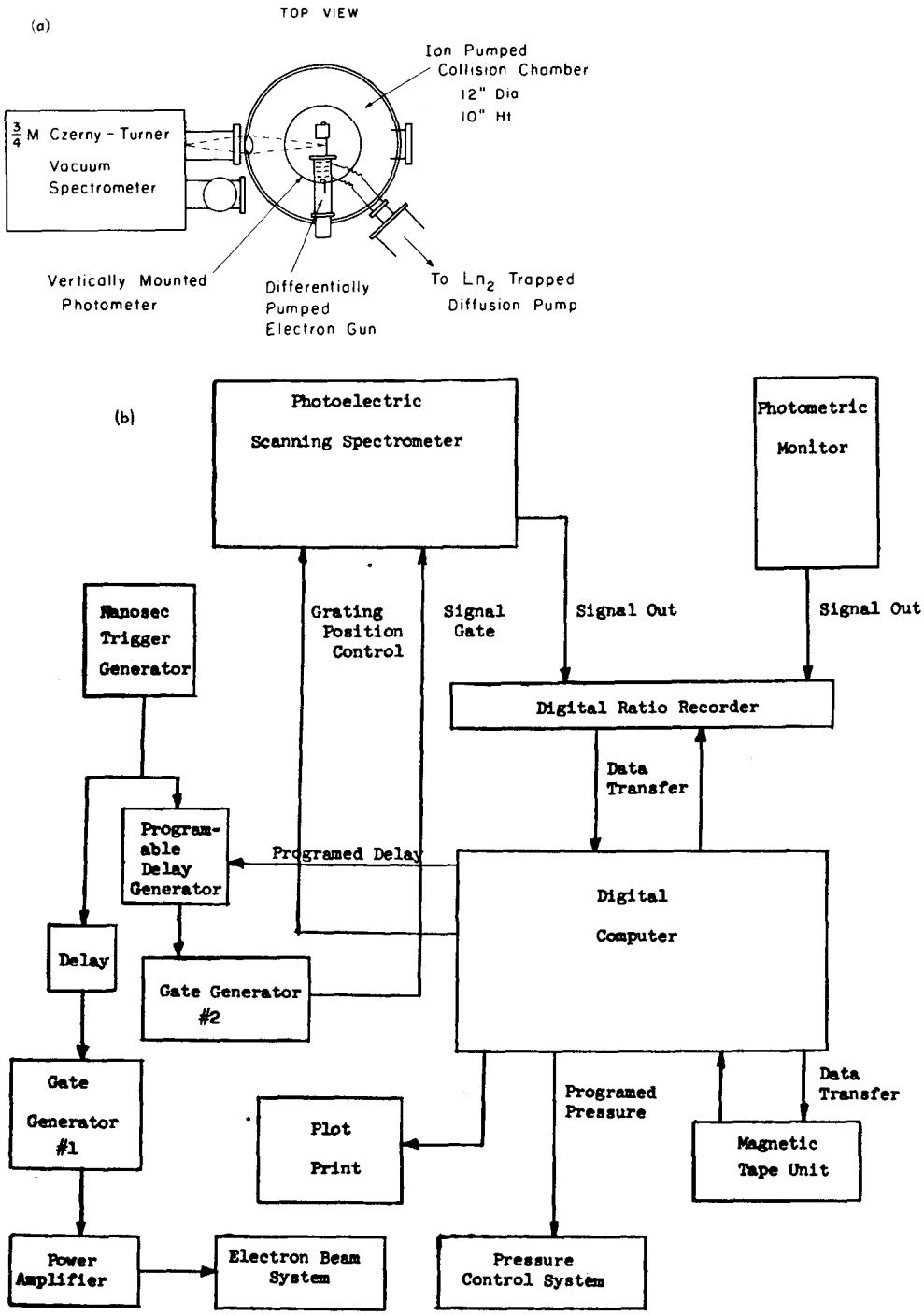

FIG. 1. Experimental system. (a) Collision chamber and observational system. (b) Control system for lifetime measurement.

mental data was ultimately stored on 9 track digital magnetic tape, and analyzed with the in-house computer.

B. Observation of transient excitation

Measurement of multiple reaction rates, such as were encountered in the present work, through observation of the response of the target gas to transient excitation, places much more stringent demands on the observational system than one encounters with species that decay with a single damping constant. Decay curves containing two or more components are very difficult to interpret in general. An analysis of such a system without knowledge of the number of separate damping components can lead to disasterous results if account is not taken of the statistical accuracy of the data as a function of time into the afterglow period. Background noise levels can also introduce large errors if not taken properly into account. In this case the data was analyzed by cross-correlating the data with an assumed decay function. The cross-correlation factor was minimized by iterative variation of the functional parameters. The magnitude of the minimized cross-correlation factor after taking into account statistical uncertainty, was then taken as a measure of the validity of the assumed decay function. The observational system described here was designed to minimize the difficulties in interpretation by generating decay curves with the same sta-

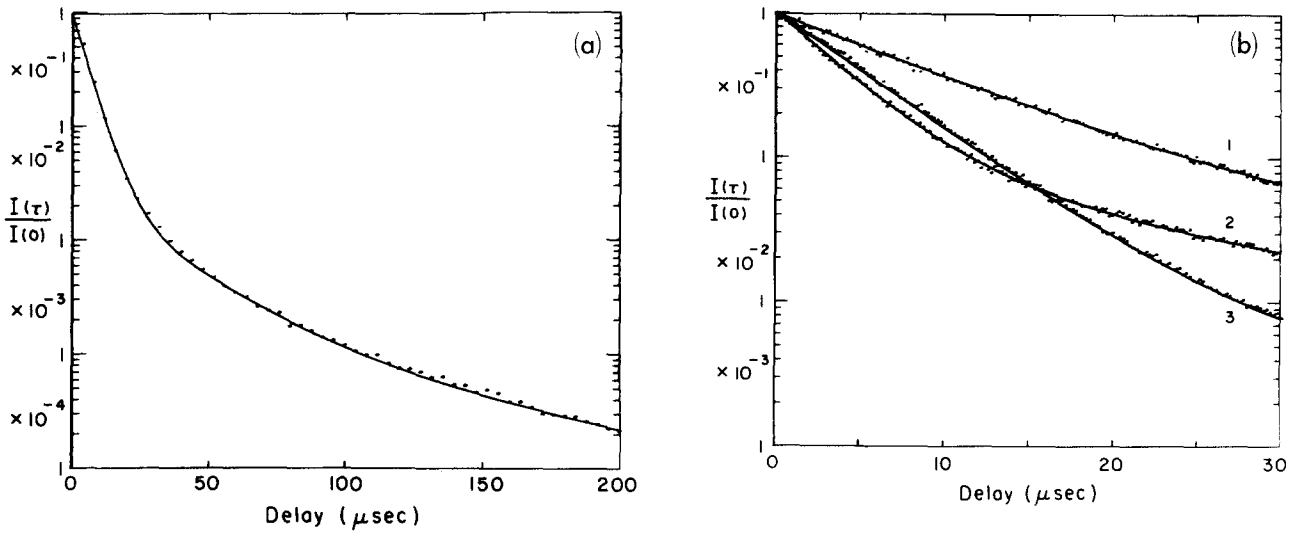

FIG. 2. Decay of N_2 $1P$ bands. Excitation function: 10 μsec excitation pulse with 210 μsec period. Smooth curve is the computed best fit three component experimental decay.

(a) (5,3) band, SP041 #036. $P=3.0$ mTorr. $E=11.0$ eV. $I=5.2$ μA peak current. $D1=0.188$ μsec^{-1}. $D2=0.410$E-1 μsec^{-1}, $I2/I1=0.23$E-1. $D3=0.118$E-1 μsec^{-1}, $I3/I1=0.118$E-1. To calculate fraction of average frequency, multiply $I(t)/I(0)$ by $f=0.19$. $\kappa=0.13$E-2.

(b) $P=10$ mTorr. 1. (12,8) band, SP043 #065. $E=12.3$ eV. $I=4.8$ μA peak current. $D1=0.262$ μsec^{-1}. $D2=0.101$ μsec^{-1}, $I2/I1=17.9$. $D3=0.375$E-2 μsec^{-1}, $I3/I1=0.446$. To calculate fraction of average frequency, multiply $I(t)/I(0)$ by $f=0.89$E-1. $\kappa=0.42$E-3.

2. (9,6) band, SP043 #053. $E=11.0$ eV. $I=3.7$ μA peak current. $D1=0.262$ μsec^{-1}. $D2=0.539$E-1 μsec^{-1}. $D3=0.392E$-3 μsec^{-1}. $f=0.11$. $\kappa=0.53$E-3.

3. (3,1) band, SP043 #013. $E=9.0$ eV. $I=4.0$ μA peak current. $D1=0.189$ μsec^{-1}. $D2=0.435$E-1 μsec^{-1}, $I2/I1=0.98$E-2. $D3=0.438$E-2 μsec^{-1}, $I3/I1=0.13$E-2. $f=0.51$. $\kappa=0.45$E-3.

tistical uncertainty for each measured point. The analysis programs could then provide cross-correlation functions of data and assumed decay functions, essentially independent of time into the afterglow. Under these conditions the cross-correlation function tends to be a direct measure of the confidence with which one may interpret the data with the assumed number of decay components. Details of the measurement technique follow.

The transient response measurements were made by pulsing the electron beam repetitively with a pulse width appropriate to the lifetime of the excited species. The signal from the photomultiplier tube was gated in phase with the pulsed electron beam and delayed with a programmable digital delay generator in order to produce a scan of signal rates as a function of time into the afterglow period (Fig. 1). The integrated signal at a given point in time into the afterglow was measured as an average period, rather than as a frequency measurement, in order to obtain uniform statistics over the afterglow period. The average period of the signal was determined by a fixed number of signal counts for each point on the decay curve. The system was stabilized against variations in pressure and electron current by using the total signal from the photomultiplier tube as an external oscillator for the period–average measurement. The points in the decay curve were thus not measured in real time, but on the basis of the magnitude of the integrated signal from the detection system required to produce 1000 counts, say, in the signal gate at a given point of time into the afterglow. The noise background for each point in the decay curve was calculated and automatically substracted in the computer. The background rate was determined by a measurement at the beginning of the program with the electron beam switched off. The subtraction of the background signal from each point on the decay curve thus required measurement of the integration time. The time measurement was obtained with a programmed time base generator connected to the computer interrupt system. Typical decay curves are shown in Fig. 2. All of the decay curves obtained in this experiment contained the same statistical scatter in the measured points. Each point represents 1000 counts of gated signal plus noise. There is very little deterioration in statistical accuracy as a function of decay time since the minimum signal to noise ratios were generally never below 10. The scatter in the measured points were generally as expected from statistical considerations. However it was occasionally necessary to interpolate points on the curves due to the introduction of noise from sources outside the laboratory. The extraneous noise sources were virtually unavoidable since most of the decay measurements at low pressure required several days of continuous operation. The measurement technique was vulnerable to systematic long period variations in background noise. However error due to this source was not detectable except on occasions of loss of temperature control in the laboratory or of the photomultiplier tube.

C. Spectral observations

Spectra of the various emissions were obtained by integrating the signal at a given grating position with the counter in the frequency mode. Instabilities in produc-

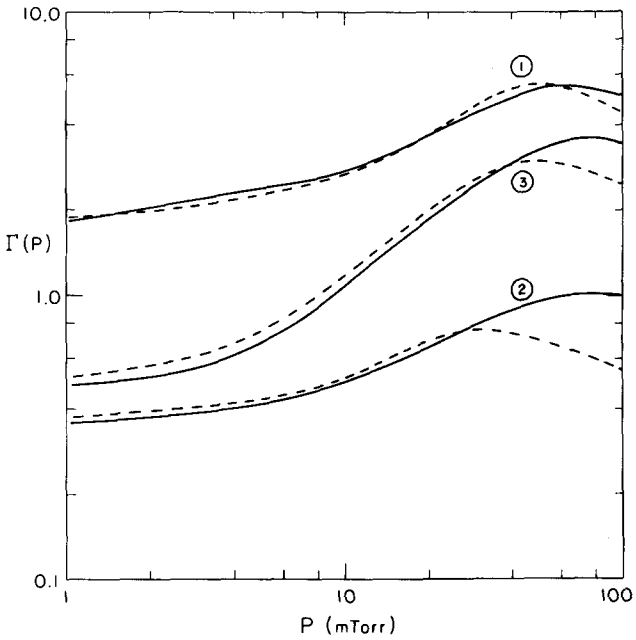

FIG. 3. Excitation efficiencies (Γ) of N_2 1P bands (see text). ——Interpolated, ----------Calculated. 1. (3,1) band, 10.8 eV 2. (9,6) band, 12.0 eV 3. (11.7) band, 12.4 eV.

tion rates were removed by monitoring the emission rate of a selected band with a filter photometer, and by applying the signal as an external oscillator to the counter, or by averaging several fast scans of the spectrometer. Spectral observations were made in both steady state and transient excitation modes. The latter was useful in determining whether or not measurements in the later periods of the afterglow were valid observations of the bands in question.

RESULTS AND ANALYSIS

A. Steady state excitation

All of the observations reported here were made with research grade N_2 in the collision chamber. Emission from all observable levels of the $B^3\Pi_g$ state, excited by 8–17 eV electrons, display a strong dependence on $[N_2]$. Figure 3 contains plots of the steady state excitation efficiency (Γ) of some of the levels as a function of pressure at energies corresponding to the peak cross sections for direct electron excitation. Γ is defined here as the ratio of emission rate to the electron flux–$[N_2]$ product ($\Gamma = I/F_e[N_2]$). The bands chosen for these measurements were carefully selected in order to avoid contamination by bands from other levels of the $B^3\Pi_g$ state. The observable bands originate from the $B^3\Pi_g\, 0 \leq v \leq 12$ levels. Higher order dependence on $[N_2]$ is detectable at pressures as low as 1–2 mTorr. The excitation efficiency (Γ) increases by factors of 3–10 between pressures at which pressure independence obtains and 100 mTorr. Part of this increase is not real due to geometric factors and there is some uncertainty due to electron scattering at the higher pressures, but the enhancement is nevertheless strong. The geometric factors were determined by a rough estimate of spacial diffusion from the lifetime measurements, and by taking into account the instrumental field of view.

There is little doubt that the estimated efficiencies can be attributed entirely to the selected N_2 1P transitions. Selection of electron energies below 11 eV removes the possibility of measurable contributions from the $C^3\Pi_u$ state. The measureable emissions longward of 5600 Å can be synthesized with bands of the $B^3\Pi_g - A^3\Sigma_u^+$ transition. Figure 4 shows a spectrum obtained at a pressure of 50 mTorr. The details of this spectrum are entirely due to the $B^3\Pi_g - A^3\Sigma_u^+$ transition in rotational thermal equilibrium (cf. Refs. 22, 23). The $B'^3\Sigma_u^- - B^3\Pi_g$ transition is absent. This transition thus appears not to be measureable under any excitation conditions at pressures below 500 mTorr (cf. Ref. 6).

B. Transient excitation

The measurements presented here were designed primarily to determine the rate coefficients for the deactivation of the $B^3\Pi_g$ state by $X\ ^1\Sigma_g^+$ molecules. For this reason most of the observations were made using a short excitation pulse, 10 μsec, with a period of about 200 μsec in order to discriminate as much as possible against the longer lived components. All of the observed levels $B^3\Pi_g\, 0 < v < 12$ contained three or more damping factors, most clearly visible in the decay of the (5, 2) band at low pressure, shown in Fig. 2. The data was analyzed with the assumption that the decay could be represented by a three component exponential function. The computation was an iterative process based on the minimization of the cross-correlation function

$$\kappa = 1 - \sum_{i=0}^{n} \alpha_i \Big/ \left[(n+1)\sum_{i=0}^{n} \alpha_i^2\right]^{1/2}, \tag{1}$$

in which

$$\alpha_i = F_i / f_i(I1, I2, I3, D1, D2, D3), \tag{2}$$

where F_i is the data set, and

$$f_i = (I1)\exp -(D1)t_i + (I2)\exp -(D2)t_i + (I3)\exp -(D3)t_i . \tag{3}$$

The factors in Eq. (3) have their usual meaning. This computational method places equal weight on each point on the decay curve in the determination of κ. The statistical uniformity of the data tends to allow a clear determination of deviations of the decay curves from the assumed functional dependence. A sum of exponential terms was assumed since three body recombination was considered a negligible factor. In any case the magnitude of the minimized κ was taken as an indicator of whether the data may contain either nonexponential factors or more than the assumed number of decay components. The accuracy of the estimated intensity factors and damping constants depends on the density of the data points, and to some degree on the relative values of intensities and damping factors. Estimates of the uncertainty in the computed results were obtained from the magnitude of κ and its sensitivity to variations in the parameters near the minimum value.

For ease of discussion we refer to the decay components as 1, 2, 3 in order of decreasing damping con-

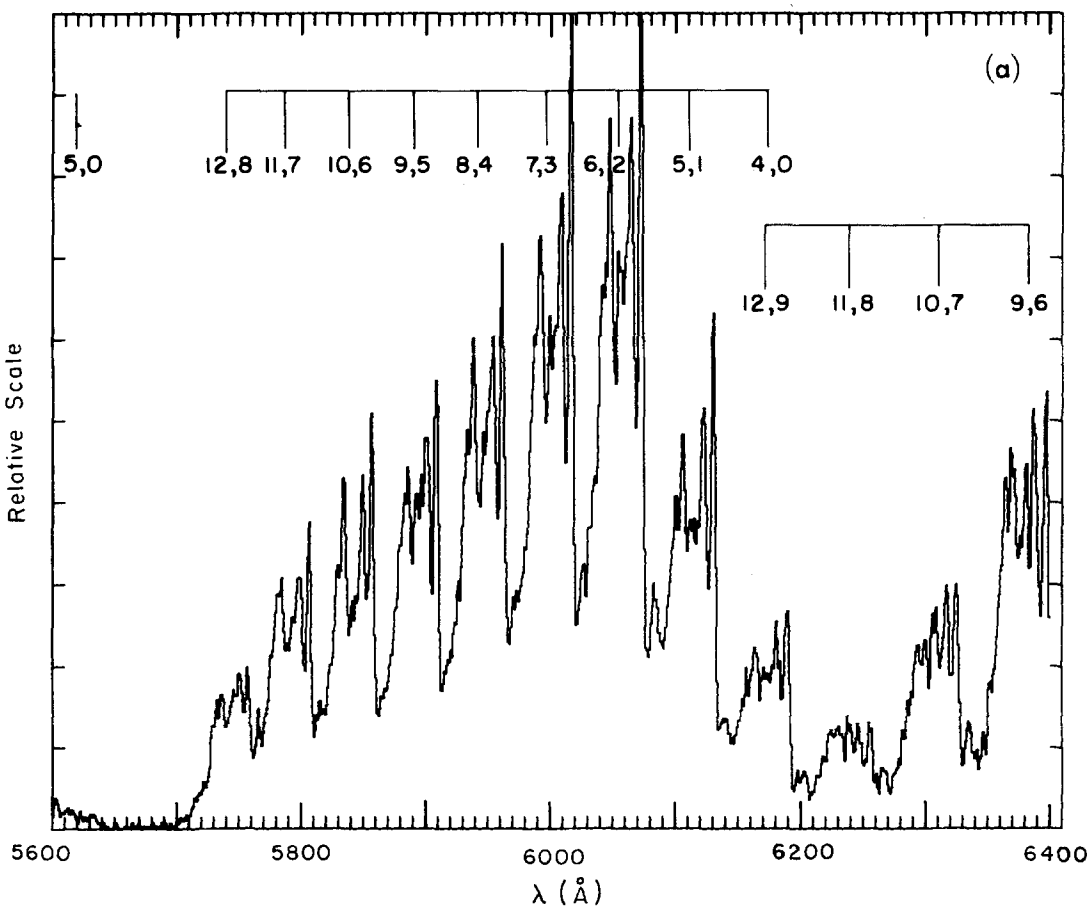

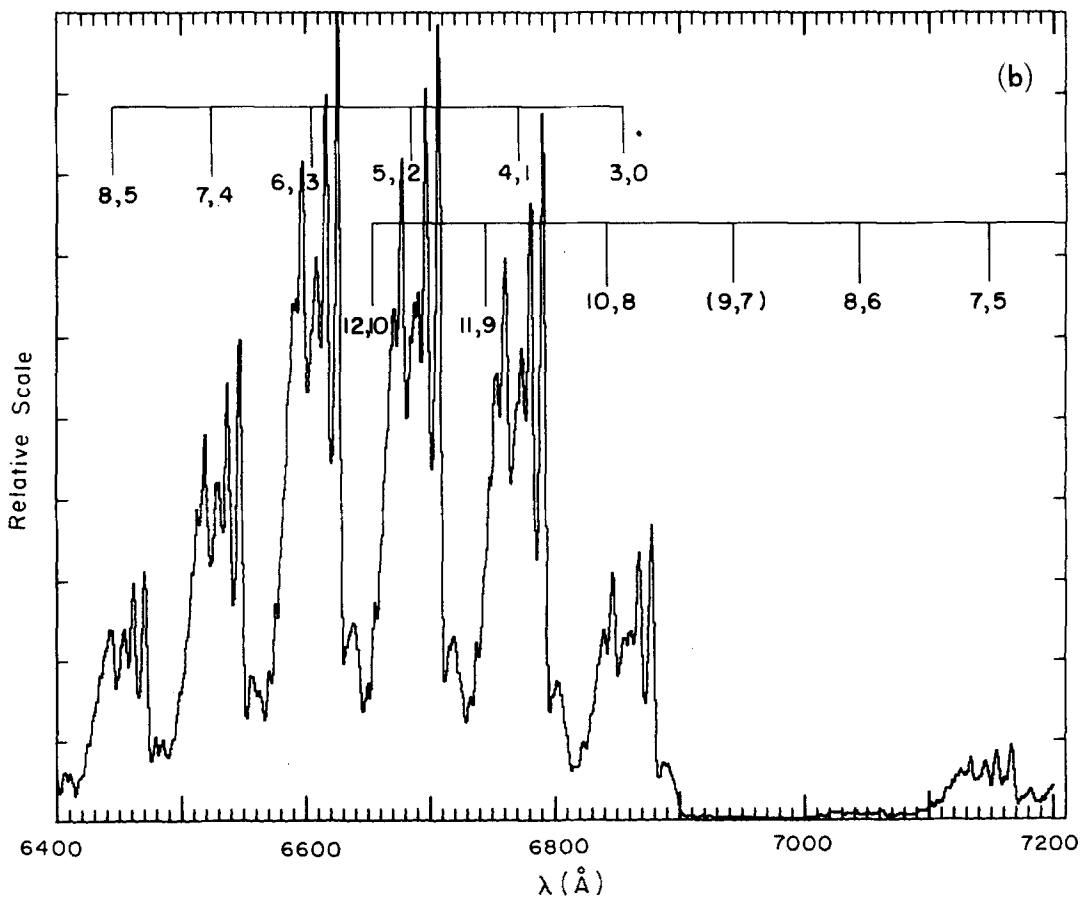

FIG. 4. N_2 1P spectrum (5600–8800 Å) (see text). $P = 70$ mTorr. $E = 10.0$ eV. $\Delta\lambda = 3.0$ Å.

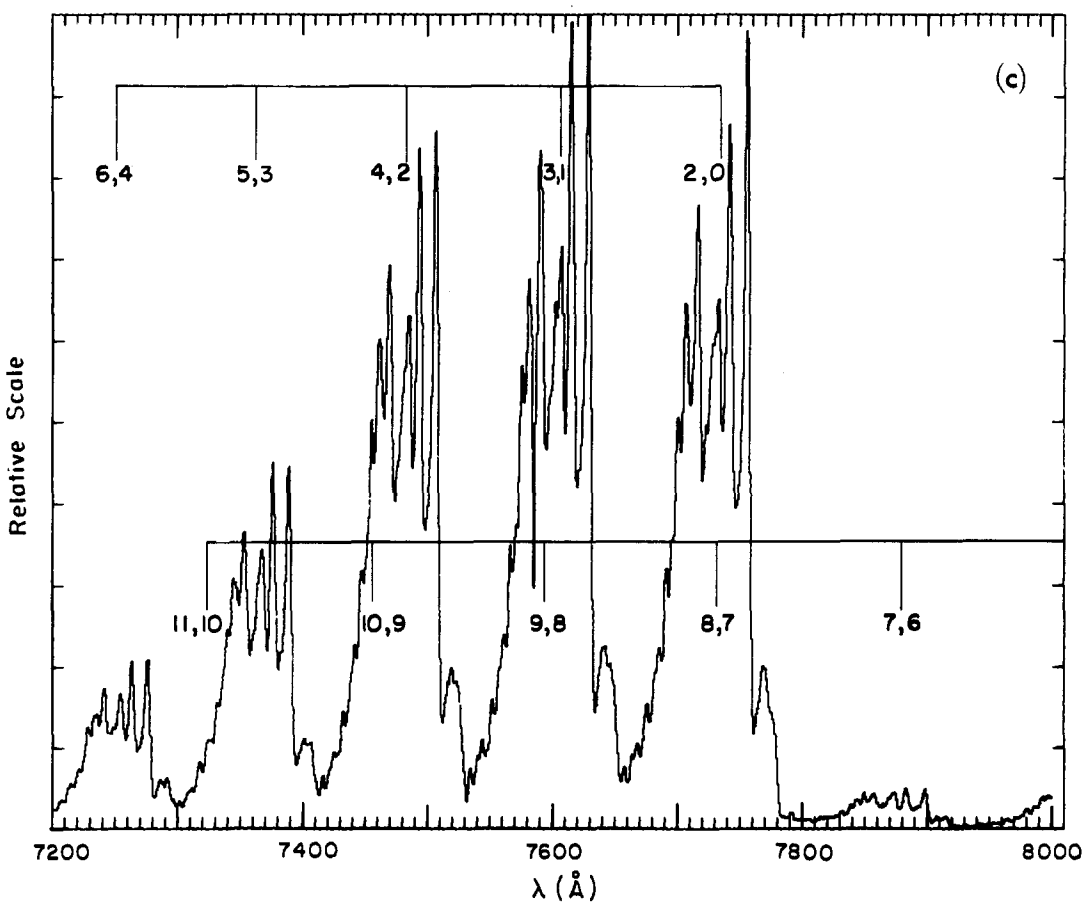

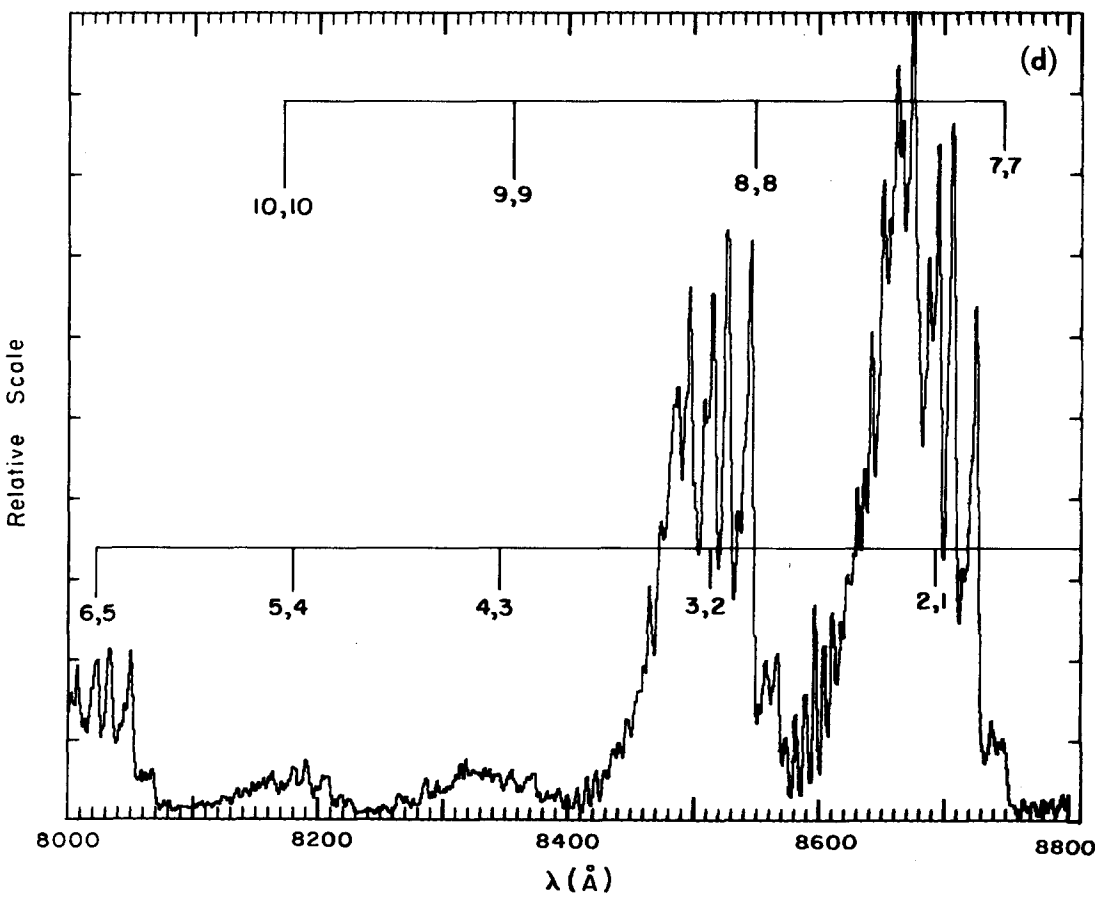

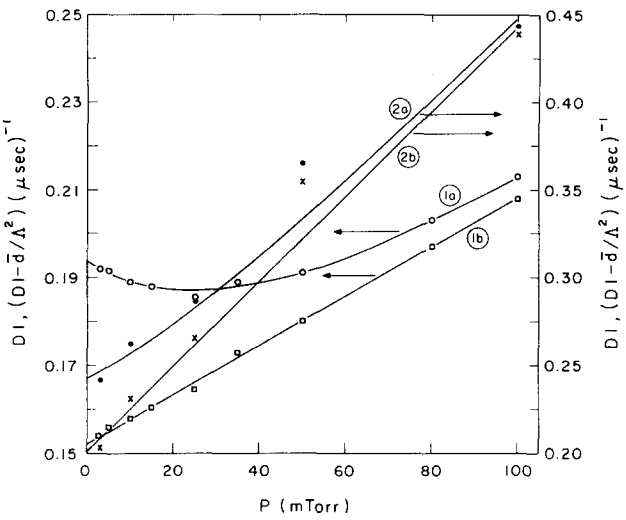

FIG. 5. 1st damping factor of N_2 1P(3,1) and (9,6) bands (see text). (3,1) band: ○-Measured values $D1(\mu\text{sec}^{-1})$. □-$(D1-\bar{d}/\Lambda^2)$. (1a)-computed $D1$. (1b)-computed $(D1-\bar{d}/\Lambda^2)$. (9,6) band: ●-Measured values $D1(\mu\text{sec}^{-1})$. x-$(D1-\bar{d}/\Lambda^2)$. (2a)-computed $D1$. (2b)-computed $(D1-\bar{d}/\Lambda^2)$.

stant. The ratios of the damping constants never pass through 1.0, as a function of pressure.

The first component

The 1st, i.e., short-lived, component of all of the $B^3\Pi_g$ levels is the only component of the set displaying an emission rate dependence 1st order or near 1st order in $[N_2]$. The remaining components are characterized by 2nd or higher order $[N_2]$ dependence. The 1st damping component was therefore identified with the intrinsic deactivation probability. The circular plotted points in Fig. 5 are the measured values of $D1$ as a function of pressure.

The pressure dependence of $D1$ for the longer lived lower vibrational levels of the $B^3\Pi_g$ state have a distinct minimum, illustrated by the plot for the $v=3$ level in the figure. This is interpreted in terms of the combined effects of diffusion and radiationless deactivation. The theoretical determination of the effect of diffusion is somewhat complicated in this case due to the complex configuration in the collision chamber caused by the intrusion of the electron gun housing and the collector. Although the diffusion coefficients for N_2 are well determined the estimated damping coefficient is complicated because, at the low pressure of the present experiment, a significant fraction of the excited molecules have heterogeneous collisions. Thus in the lower pressure region the diffusion loss probability tends to be pressure independent. The diffusion loss function was estimated by assuming that the following approximation holds with sufficient accuracy.

$$\frac{\bar{d}}{\Lambda^2}=\frac{d1}{\Lambda^2}\exp-[N_2]\chi+\frac{d2}{\Lambda^2[N_2]}(1-\exp-[N_2]\chi)\ , \qquad (4)$$

where $d1/\Lambda^2$ represents the collision free loss probability, $d2/\Lambda^2$ the loss probability for molecules controlled by homogeneous collisions, and χ is the cross section transport-length product determining the probability of collision free loss. Λ is a characteristic length determined by the configuration of the collision chamber (cf. Hasted[24]). At high pressures Eq. (4) reduces to $\bar{d}/\Lambda^2=d2/\Lambda^2[N_2]$, and $d2$ thus corresponds to the measured (cf. Ref. 25) homogeneous diffusion coefficient. At low pressures time of flight to the walls tends to determine the loss rate. Equation (4) can be considered only a rough approximation since one may expect an altered velocity distribution in the excited species at low pressures.

For the present purpose the equation provides a satisfactory fit (Fig. 5) to the shape of the deactivation probabilities, with values of the parameters which appear to be reasonable in terms of the chamber geometry. The parameters in Eq. (4) were estimated with a 4 variable best fit to the observed variation of $D1$ for the (3,1) band, shown in Fig. 5. The curve drawn through the observed points is the calculated deactivation function. The square points in the figure are the values $(D1-\bar{d}/\Lambda^2)$. The derived values of the parameters in Eq. (4),

$$d1/\Lambda^2=0.024\ \mu\text{sec}^{-1}\ ,$$

$$d2/\Lambda^2=1.45\text{E}13\ \mu\text{sec}^{-1}\cdot\text{cm}^{-3}\ ,$$

$$\chi=1.18\text{E}-15\ \text{cm}^3\ ,$$

were used in the reduction of all of the deactivation probability measurements.

Assuming the region between the face of the electron gun housing and the collector form an approximation to a cylinder with infinite radius, the effective length obtained from $d2/\Lambda^2$ using the $A\ ^3\Sigma_u^+$ diffusion coefficient of Ref. 25, we obtain the effective distance between collector and housing of 1.75 cm compared to an actual separation of 1.5 cm. Thus most of the loss is accounted for in terms of the fundamental mode diffusion of a gas between two infinite plane surfaces.

The zero pressure limit yields $\bar{d}/\Lambda^2=0.041\ \mu\text{sec}^{-1}$. If we assume an equilibrium cosine population distribution between the housing face and collector, with a surface deactivation efficiency $\gamma=1$, the effective length based on the mean velocity at 300 °K becomes $L=1.8$ cm at the zero pressure limit. This again is a reasonable value.

Plots of $(D1-\bar{d}/\Lambda^2)$ should and do yield linear pressure dependence for all of the first decay components of the $B^3\Pi_g$ state. The slope of the $(D1-\bar{d}/\Lambda^2)$ curves are thus interpreted in terms of N_2X deactivation, and extrapolation to zero pressure yields the radiative deactivation probability, A_v. Table I shows the measured rate coefficients of the $B^3\Pi_g$ state, in comparison with other measurements. The variation of the probable errors given in the table is due partly to variation in the ability to experimentally discriminate against the afterglow components at the higher pressures, and partly to a reduced sensitivity of the cross-correlation factor to variations in the estimated probabilities. It was possible to discriminate against the longer lived components of the lower levels up to $v=10$ by reducing the electron energy to values a fraction of a volt above threshold. This reduced the afterglow components an

TABLE I. Rate coefficients for $N_2 B\ ^3\Pi_g$ deactivation by $N_2 X^1\Sigma_g^+$. Units: 10^{-11} cm^3 sec^{-1}.

V	0	1	2	3	4	5	6	7	8	9	10	11	12
$k_2^{v\,a}$	~1[d]	~1[a]	1.9±0.2	1.7±0.2	1.8±0.2	2.3±0.2	4.1±0.4	6.6±0.4	7.2±0.4	9.8±1	6.3±0.8	2.0±0.3	$1^{+1}_{-0.5}$
$k_2^{v\,b}$						6	4	5	6	6	4	4	0.8
$k_2^{v\,c}$										0.9	2.8	7.2	11

[a]Present work.
[b]Calculated from Jeunehomme and Duncan[12] data.
[c]Becker *et al.*,[6] from low pressure L–R afterglow.
[d]Very uncertain estimates from steady state observations.

order of magnitude relative to the direct excitation process for some of the lower $B\ ^3\Pi_g$ levels. It was not possible to produce the same effect in the case of the $v=11$, 12 levels. The reduction of the measurements on the $v=6$, 7 levels appeared to pose a special problem, due to a noticeably reduced sensitivity to variations in the parameters and a generally larger cross-correlation coefficient, 5E−4−7E−4, compared to 3.5E−4−5E−4 for the other bands of the system. The difficulty was not statistical in nature, since repeated measurements produced about the same results. There was no evidence that other states or levels at the same wavelengths were contaminating the decay curves. This will be discussed further in the next section.

Figure 6 shows a plot of the estimated $B\ ^3\Pi_g$–$A\ ^3\Sigma_u^+$ transition probabilities in comparison with the values calculated by Refs. 20, 22. The agreement is within 10%. The $B\ ^3\Pi_g$ state transition probabilities have been measured on numerous occasions and there is very good agreement on the whole, beginning at about the time of the Ref. 12 measurements (cf. Ref. 22).

The second component

The second damping constants of all of the observed levels appear to be diffusion limited at the low pressure limit of the observations. There is some scatter in the results at low pressure because the excitation conditions were designed to discriminate against the longer lived components. Figure 7 shows plots of $(D2-\bar{d}/\Lambda^2)$ for some of the $B\ ^3\Pi_g$ levels. According to the discussion below, the dominant source of the second decay components must be the higher levels of the $A\ ^3\Sigma_u^+$ state.

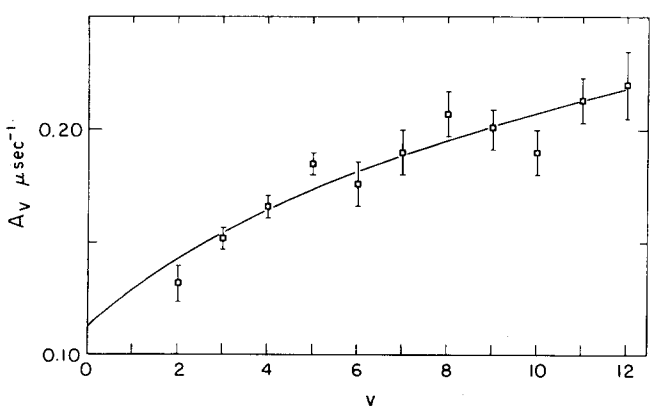

FIG. 6. Radiative probabilities of $N_2\ B\ ^3\Pi_g$ levels. Smooth curve due to calculation by Ref. 22. □-Present work. See Ref. 22 for other measurements.

The plotted $(D2-\bar{d}/\Lambda^2)$ points are linear in $[N_2]$ with the exception of the $B\ ^3\Pi_g\ v=6, 7, 9, 11, 12$ levels. All of the exceptions have a characteristic declining rate of change of deactivation rate with increasing $[N_2]$, as shown for the (9, 6) band in Fig. 7. This clearly raises difficulties in interpretation, but the rate coefficients for $[N_2 X]$ deactivation were determined from the estimated asymptotic value at the low pressure end of the measurements. The argument for making this assumption will be given in the following section.

Table II gives the estimated rate coefficients for the observed levels. The $(D2-\bar{d}/\Lambda^2)$ curves extrapolated to zero pressure all intersect at slightly positive values of $(D2-\bar{d}/\Lambda^2)$. The intercepts are not judged to be significant since they are almost at the noise level.

Curves of $(I2/I1)$ as a function of pressure are shown in Fig. 8, with an example of energy dependence for one of the levels. The dashed lines are calculated curves, discussed in the following text. The plotted ratios have been corrected for the experimental integration of Eq. (3).

The ratio of the emission rates of the second decay components relative to the first were sensitive to the electron energy to varying degrees at a given pressure, for all of the observed levels. It was possible to suppress the second components of most of the $B\ ^3\Pi_g$ levels by an order of magnitude by reducing the electron energy to near threshold values. However, this was not true

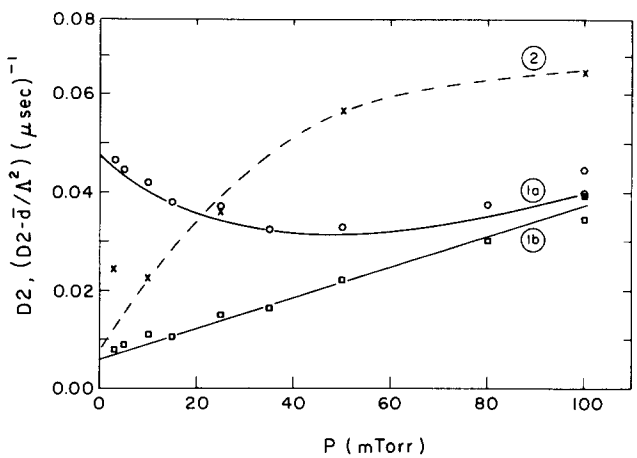

FIG. 7. 2nd damping factor of N_2 IP(3.1) and (9, 6) bands (see text).
1. (3,1) band: ○, measured values $D2(\mu\text{sec})^{-1}$. □, $(D2-\bar{d}/\Lambda^2)$. (a) computed D_2. (b) computed $(D2-\bar{d}/\Lambda^2)$.
2. (9,6) band: x, measured values $(D2-\bar{d}/\Lambda^2)\ (\mu\text{sec})^{-1}$. —— interpolated curve.

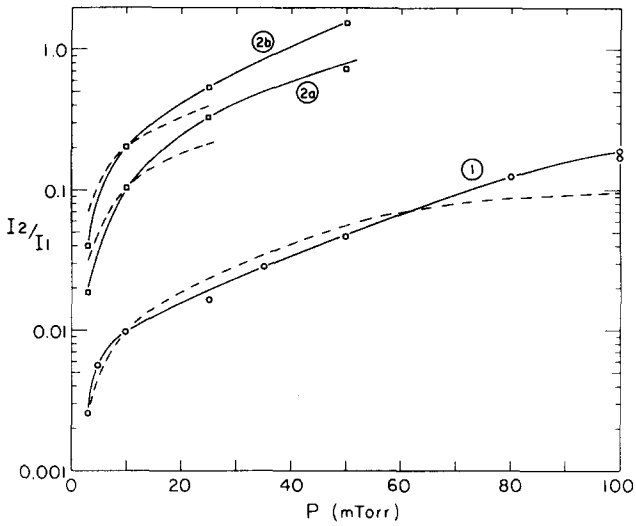

FIG. 8. Intensity ratios $I2/I1$ of N_2 1P decay components (see text). ——Interpolated, ----------Calculated.
1. (3,1) band: 9.0 eV. $\sigma A_3 = 2.2E\text{-}18\ cm^2$.
2. (6,3) band: (a) 9.0 eV. $\sigma A_6 = 1.9E\text{-}18\ cm^2$. (b) 10.5 eV. $\sigma A_6 = 3.7E\text{-}18\ cm^2$.

of the $v=11$, 12 levels, in which variation of the second component appeared to be no more than a factor of 2 at near threshold energies. At energies greater than the peak cross section for direct excitation of the $B\ ^3\Pi_g$ state, the second component also appeared to decline, but more moderately. The long integration times required for the measurements did not allow a good definition of the shape of the second component cross sections, however, they all were narrower to varying degrees than the corresponding direct $B\ ^3\Pi_g - X\ ^1\Sigma_g^+$ cross sections, with peak values in near energy concidence (~1 eV) with the direct process.

The third component

The third component of the $B\ ^3\Pi_g$ decay curves was very weak and longer lived than one would estimate from diffusion losses as estimated from Eq. (4). The estimated $I3/I1$ ratios at low pressures were generally uncertain and in the region of 10^{-3}–10^{-5}. No well defined pressure dependence could be established, but it appeared to be second or higher order in $[N_2]$. Pressure dependence of the relative emission rate of this component displayed a rough correlation to that of the second component. The deactivation probabilities were about the same order for most of the levels at a given pressure, and varied from ~1.2E4 sec^{-1} at 3 mTorr to ~1E3 sec^{-1} at 100 mTorr. Table III provides a comparison of $I3/I1$ ratios and $D3$ values obtained at 10 mTorr. The $I3/I1$ ratios are not strictly comparable to one another since the measurements were made at energies that did not coincide with the cross-section peaks. However it is clear that the $v=12$ level is most heavily populated by the third component on a relative basis, by an order of magnitude. Other levels receiving significant contributions are $v=11$, 6, 4, 2, 1. According to the discussion below, one possible source for the third component, if it is the same source for all levels, may be energy pooling of the lower $A\ ^3\Sigma_g^+$ levels. This could occur in the outer volume of the collision chamber beyond the region between the electron gun housing and collector where the diffusion loss probability would be low enough to make it unnecessary to involve diffusion suppresion as an explanation of the long lifetime; the region between gun housing and collector represents a diffusion rate too large to explain the observed low loss rates. Figure 9 shows a plot of the $C\ ^3\Pi_u - B\ ^3\Pi_g$, N_2 2P(0, 0) band decay showing a third component having about the same long lifetime as the third component of the N_2 1P bands. It is possible that all may have the same source, $A\ ^3\Sigma_u^+ v=0, 1$ molecules.

DISCUSSION

We consider the following reactions in this discussion.

$$N_2X + e \rightarrow (N_2B, N_2A, N_2C) + e\ , \tag{R1'}$$

$$N_2A + N_2X \rightarrow N_2B + N_2X\ , \tag{R1}$$

$$N_2B + N_2X \rightarrow N_2^*X + N_2^{**}\ , \tag{R2}$$

$$N_2A + N_2X \rightarrow N_2^*X + N_2^{**}\ , \tag{R3}$$

$$N(^4S) + N_2A \rightarrow N_2^* + N^*\ , \tag{R4}$$

$$N + N + N_2X \rightarrow N_2A + N_2^*\ , \tag{R5}$$

$$N + N + \text{surface} \rightarrow N_2^*\ , \tag{R6}$$

$$N + N + N_2X \rightarrow N_2^* + N_2^*X\ , \tag{R7}$$

$$N_2A + \text{surface} \rightarrow N_2^*X\ , \tag{R8}$$

$$N_2B + \text{surface} \rightarrow N_2^*X\ , \tag{R8'}$$

$$N_2A(v=0,1) + N_2A(v=0,1) \rightarrow N_2^* + N_2^*X\ , \tag{R9}$$

$$N_2A(v=0,1) + N_2A(v=0,1) \rightarrow N_2B + N_2^*X\ , \tag{R10}$$

$$N_2A(v=0,1) + N_2A(v=0,1) \rightarrow N_2C + N_2^*X\ , \tag{R11}$$

$$N_2\ ^5\Sigma_g^+ + N_2X \rightarrow N_2B(v=12) + N_2X\ . \tag{R12}$$

The kinetics of the N_2 $B\ ^3\Pi_g$ state are clearly of prime importance to any theory of the N_2 afterglow. The question of whether one can accept the relative emission rates from the $B\ ^3\Pi_g$ levels as a reflec-

TABLE II. Rate coefficients for N_2 $A\ ^3\Sigma_u^+$ deactivation by N_2 $X\ ^1\Sigma_g^+$. Units: $10^{-11}\ cm^3\ sec^{-1}$.

$A\ ^3\Sigma_u^+ v$[a]	10	11	13	14	16	17	19	21	22,23	24,25	26,27
$B\ ^3\Pi_g$	2	3	4	5	6	7	8	9	10	11	12
$k_3 v$	1.0±0.15	8.8±0.7	2.0±0.3	2.0±0.3	$4^{+1}_{-0.5}$	$5^{+2}_{-0.5}$	1.9±0.3	$3.0^{+0.7}_{-0.3}$	$3.5^{+0.7}_{-0.3}$	$4.5^{+1}_{-0.4}$	5^{+2}_{-1}

[a]Labeled according to energy coincidence with $B\ ^3\Pi_g$ levels.

tion of relative production rates, and whether vibrational relaxation plays a part in the population distribution, are critical to the determination of which of the possible energy transfer processes are operating.

According to the present work there is considerable variation in the rate coefficients of R2 (Table I) which give rise to relative production rates significantly different from the observed relative $B\ ^3\Pi_g$ $v=0-12$ emission rates. Other measurements that are directly comparable are shown in the table. The estimates calculated from data given by Ref. 12 can be regarded as comparatively rough since they are taken from measurements at only two points in pressure. Reference 12 for this reason did not detect the variation in lifetime observed in later work by Jeunehomme[26] in an NO : N_2 mixture. Thus it is not surprising that agreement is only within a factor of 2. However, there is some indication that the envelopes of the variation as a function of v are comparable. There is spectacular disagreement with the Ref. 6 estimates which, unlike the present and Ref. 12 measurements, were made in an L–R afterglow in the 0.5–500 mTorr region. The Ref. 6 estimates of k_2 are an order of magnitude larger at $v=12$ and an order of magnitude less at $v=9$. These values were obtained from two parameter fits to observations of a static system under steady state excitation. The source of the discrepancy is not obvious. The Ref. 6 reaction chamber was a 7.5 m diameter stainless steel sphere. It is possible the energy pooling reaction R9 may thus have some significant effect on their observations even in the low pressure region, because loss of N_2A molecules would never be diffusion limited in the observational pressure range. The contribution of R10 to N_2B production depends on the degree of dissociation and on the value of k_4 (cf. Ref. 21). If R10 were significant, the calculated value of k_2 on the basis of a two parameter fit would tend to be a lower limit. This would not explain the high value for $k_2 12 (v=12)$, and probably would not be significant enough to explain the low value of $k_2 9$ relative to the present estimates. Other estimates of k_2 by Refs. 9 and 27, 3E – 11 – 4E – 11 cm^3sec and 2.7E – 11 cm^3sec^1, respectively, are averages over a number of bands and not directly comparable to the numbers in Table I. However the magnitudes appear to be in reasonable agreement with the present estimates. The coefficients for R5 were calculated assuming the N_2B populations to be controlled by reactions R1, R2, R3, R5 in the steady state. This reduces to

$$IB_v = [N]^2 AB_v k_5 v k_1 v / k_2 v k_3 v \ , \tag{5}$$

at pressures above 1 Torr, where IB_v is the volume emission rate of level v, AB the radiative transition probability, and [N] is the atomic nitrogen concentration. According to Ref. 5 the quantity

$$\sum_v AB_v k_5 v k_1 v / k_2 v k_3 v = 1.4\text{E} - 17 \ \text{cm}^3\text{sec}^{-1} \ ,$$

at pressures above 1 Torr. Table IV shows the relative N_2B emission rates from the Ref. 2 and Ref. 6 data normalized at $v=11$, and the values of k_5 calculated using the new values of k_2. Recombination into the N_2A state (k_5) was estimated using the Ref. 22 values of AB, the present values of k_2, and by assuming that every deactivating collision of $N_2A_v > 6$ resulted in production of N_2B molecules ($k_1 = k_3$). This may not be strictly correct according to the evidence given here and the discussion below. Hence the totals $\sum k_5 v$ given in Table IV should be considered lower limits, although we do not expect the real values to be significantly higher. According to the totals given in Table IV the fraction of atomic nitrogen recombinations ending in $B\ ^3\Pi_g$ production is about 25%. This is lower by a factor of about 2 than an earlier estimate[19] based on a constant $k_2 = 7\text{E} - 11$ cm^3sec^{-1}. The distribution of $k_5 v$ values in Table IV reflects a much more uniform distribution in production of N_2B levels than obtains from a uniform k_2. This tends to suggest, at least, an intervening nonresonant process. The order of magnitude differences in the relative emission rates at low v as listed in Table IV are somewhat disturbing. The Ref. 6 results appear to indicate that most of the energy is delivered to N_2B $v<4$. The Ref. 2 results have been generally accepted up to this point. We tentatively accept the Ref. 2 measurements here pending further evidence to the contrary.

The question of whether the $B\ ^3\Pi_g$ state suffers vibrational relaxation on collisions with N_2X is of some importance to theories of the afterglow involving the $^5\Sigma_g^+$ state (cf. Refs. 2, 11, 28, 29). According to the evidence obtained here the rate of R2 is dominated by electronic deactivation. The argument for this is as follows. The relaxation from one level to another, excluding other processes that may enter can be described by

$$\frac{d[N_2B]}{dt} = -[N_2B_v]DB_v + [N_2B_{v+n}][N_2X]k \ , \tag{6}$$

where DB_v in the deactivation probability of molecules

TABLE III. Third decay component of $B\ ^3\Pi_g$ state at 10 mTorr.[a]

v	1[b]	2	3	4	5	6	7	8	9	10	11	12
$I3/I1$	1.4 – 2[c]	9 – 3	1.2 – 3	5 – 3	2 – 5	5 – 3	2 – 4	7 – 4	2 – 3	2 – 3	1.3 – 2	4.4 – 1
$D3$ (μsec^{-1})	9 – 3	7 – 3	4 – 3	5 – 3	4 – 3	9 – 3	4 – 3	5 – 4	4 – 4	7 – 3	7 – 3	4 – 3
E(eV)	14.4	9.0	9.0	8.7	9.0	9.0	10.5	10.5	11.0	11.5	12.0	12.3

[a] See text.
[b] This level contains significant contribution from $C\ ^3\Pi_u$ long lived component.
[c] $1.4 - 2 = 1.4 \times 10^{-2}$.

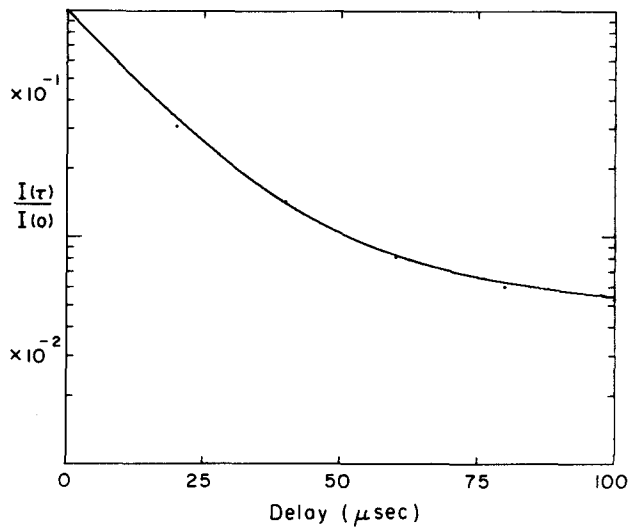

FIG. 9. Decay of N_2 2P (0,0) band, SP055 #018. $P=10$ mTorr $E=14.2$ eV. $I=4.0$ μA peak current. $D2=0.635\text{E-}1$ μsec^{-1}. $D3=0.414\text{E-}2$ μsec^{-1}, $I3/I2=0.29\text{E-}1$. To calculate fraction of average frequency multiply $I(t)/I(0)$ by $f=0.81\text{E-}3$, $\kappa=0.52\text{E-}3$. Note that although the system is capable of measuring $D1\approx 2.2\text{E}+1$ μsec^{-1}, it is not possible with the wide integration gate utilized in this case.

N_2B_v, and k is the rate coefficient for production of N_2B_v by relaxation of N_2B_{v+n}.

Assume the decay of N_2B_{v+n} to be a simple exponential,

$$N_2B_{v+n}=[N_2B_{v+n}]_0\exp-(DB_{v+n})t\ , \tag{7}$$

Eq. 6 then reduces to

$$[N_2B_v]=\left\{[N_2B_v]_0-\frac{[N_2B_{v+n}][N_2X]k}{(DB_v-DB_{v+n})}\right\}\exp-(DB_v)t + \frac{[N_2B_{v+n}][N_2X]k}{(DB_v-DB_{v+n})}\exp-(DB_{v+n})t\ . \tag{8}$$

If DB_v and DB_{v+n} tend toward equality, Eq. (8) is indeterminate and Eq. (6) reduces to

$$[N_2B_v]=\{[N_2B_v]_0+[N_2B_{v+n}]_0[N_2X]k(t)\}\exp-(DB_v)t\ , \qquad DB_v=DB_{v+n}\ . \tag{9}$$

Thus relaxation within the $B\ ^3\Pi_g$ state would result in decay characterized by two exponential components with nearly equal damping constants [Eq. (8)] or in a single exponential component with a time dependent amplitude term [Eq. (9)]. The analysis program would recognize only one decay component in either case, but with a cross-correlation coefficient larger than normal and less sensitive to perturbations of the estimated decay parameters, due to apparent distortion of the decay curve represented by Eqs. (8) and (9). The separation of the damping constants in the three component analysis of the present observations is a minimum factor of 2. Thus any vibrational relaxation within a population controlled by radiative deactivation would appear as a perturbation of the corresponding damping constant due to the near equality of the N_2B_{v+n} damping constant. If the product $[N_2X]k$ (cf. Eq. 9) is comparable to DB_v, significant deviations of the decay component from that of a single exponential curve would occur in the early decay period. This would give rise to a reduction in sensitivity of κ to perturbations of the decay parameters, too large to be accounted for by noise, and tend to produce an apparent nonlinear pressure dependence of $(DB_v-\bar{d}/\Lambda^2)$. Decreased sensitivity of κ does occur for $N_2B\,v=6$, 7 levels, but the $(D1-\bar{d}/\Lambda^2)$ components appear to be linear in $[N_2]$. It is in fact the $(D2-\bar{d}/\Lambda^2)$ components of these levels that display a nonlinear $[N_2]$ relationship (Fig. 6). If vibrational relaxation were to be a significant component of R2 we require a minimum $k=1\text{E}-11$ cm^{3}sec^{-1}. This would give rise to measureable deviations of the $D1$ components of the lower levels of the N_2B state in the 40–100 mTorr region. Such deviations have not been observed. Other evidence indicating that R2 is mostly due to electronic deactivation appears in the Ref. 7 work. DeMonchy,[7] using a discharge tube cleaned by molybdenum sputtering, displayed spectra of an afterglow in pure N_2 at 1.8 Torr showing differential decay of the N_2 1P bands. In the late afterglow the $N_2B\,v=10$, 11, 12 emission rates remained at a significant level with no measureable emission from the lower levels. Whatever the source mechanism may be in this case, this suggests that the N_2B relaxation rate in pure N_2 does not compete with electronic deactivation.

The $A\ ^3\Sigma_u^+$ state appears to be the only viable candidate as the source for the second decay component of the N_2B levels. This conclusion is based on a number of factors. The excitation functions of the second components are approximately coincident in energy with those of the $B\ ^3\Pi_g$–$X\ ^1\Sigma_g^+$ transition. The shapes of the function are somewhat narrower than the corresponding lower N_2B levels (see Fig. 8).

According to the estimates obtained here the total electron cross section of the source must be a factor of

TABLE IV. Relative emission rates from $N_2\,B^3\Pi_g$ levels and calculated recombination rate coefficients (k_5).[a]

v	0	1	2	3	4	5	6	7	8	9	10	11	12	Σv
IB_v[c]	45	27	40	14	10	9.8	14	4.2	3.3	2.7	9.3	35	15	229
IB_v[d]	(500)[b]	368	188	66	42	35	31	15	6	7	13	35	17	1324
$k_5{}^{v}$[c] cm^{6}sec^{-1}	(1–34)[b]	(1–34)[b]	3.3–34	9.6–35	6.8–35	7.9–35	1.9–34	9.0–35	7.4–35	8.0–35	1.7–34	2.1–34	4.2–35	1.7–33
$k_5{}^{v}$[c] cm^6 sec^{-1}	(2–34)[b]	(3–34)[b]	2.7–34	7.9–35	5.0–35	4.9–35	7.5–35	5.6–35	2.3–35	3.6–35	4.2–35	3.5–35	8.2–36	1.2–33

[a]See text.
[b]Extrapolated.
[c]Calculated from Bayes and Kistiakowsky[2] data, pure N_2, $P=4$ Torr.
[d]Calculated from Becker *et al.*[6] data, pure N_2, $P=5$ Torr.

about 3 larger than the $B\,^3\Pi_g$–$X\,^1\Sigma_g^+$ value. This, coupled with the second order dependence of these components, suggests a resonance type collision transfer process from a set of vibrational levels. The narrow extent in energy of the excitation functions is typical of electron exchange processes. The production of N_2B molecules by the second order reaction is still measurable at energies as low as 8.2 eV. These factors tend to eliminate any of the singlet states as possible sources. The only viable prospect for this is the $A\,^3\Sigma_u^+$ state. The $W\,^3\Delta_u$ state can be eliminated as a precursor to the $B\,^3\Pi_g$ state on several grounds. Saum and Benesch[30] (cf. Ref. 31) have observed an infrared transition in 2–10 Torr of N_2 identified as the W–B transition. If the vibrational numbering is correct the W and B potential curves must be very close together. There is no sign of the W–X transition in electron energy loss spectra[32,33] at comparable electron energies. A theoretical estimate of the electron cross section[34] is two orders of magnitude smaller than we require here. The W state can be populated by radiative transitions from the B state but the branching ratio, B–W/B–A, must be very small if we use the estimates of $B\,^3\Pi_g$ lifetimes $(B-W+B-A)$ in the present work in comparison with the measured B–A probabilities.[35] This tends to place the $W\,^3\Delta_u$ production rates at a level far too low, under the present excitation conditions, to be considered seriously.

The $B'\,^3\Sigma_u^-$ state with threshold 8.2 eV, does not have a measureable electron cross section. The B'–B transition is observed only in the afterglow at pressures above 1 Torr. The $A\,^3\Sigma_u^+$ state on the other hand has an electron excitation cross section comparable to the $B\,^3\Pi_g$ cross section according to estimates made from electron energy loss spectra[21a,36] and some molecular beam measurements.[37,38] In addition the Franck–Condon factors for the A–X transition predict a uniform excitation cross section over the higher vibrational levels required by the observation of secondary B state production.

The steady state measurements of excitation efficiency are analyzed with the assumption that reactions R1′, R1, R2, R3 are the controlling factors. The excitation efficiency, ΓB, of the B state then reduces to

$$\Gamma B_v = (\sigma B_v/DB_v)(1+(\sigma A_v/\sigma B_v)\{[N_2]k_1v/(k_8+[N_2]k_3v)\}), \quad (10)$$

where

$$DB_v = AB_v + k_{8'} + [N_2]k_2 ,$$

σ is the excitation cross section, and AB_v is the $B\,^3\Pi_g$ radiative transition probability. AA_v, the transition probability of the $A\,^3\Sigma_u^+$ state, is too small to enter and has been neglected. A term containing the contribution to the A state by the B–A transition has not been included. It can be shown that this term does not contribute significantly to the higher A state levels involved in reaction R1. The ratio $(\sigma A_v/\sigma B_v)$ is obtained from the measurements shown in Fig. 3 by application of the R2 and R3 rates measured in the transient excitation measurements. Equation (10) cannot be applied directly to the observations because the emitting volume is not the same for the various N_2B production mechanisms. In addition electron scattering makes the excitation volume

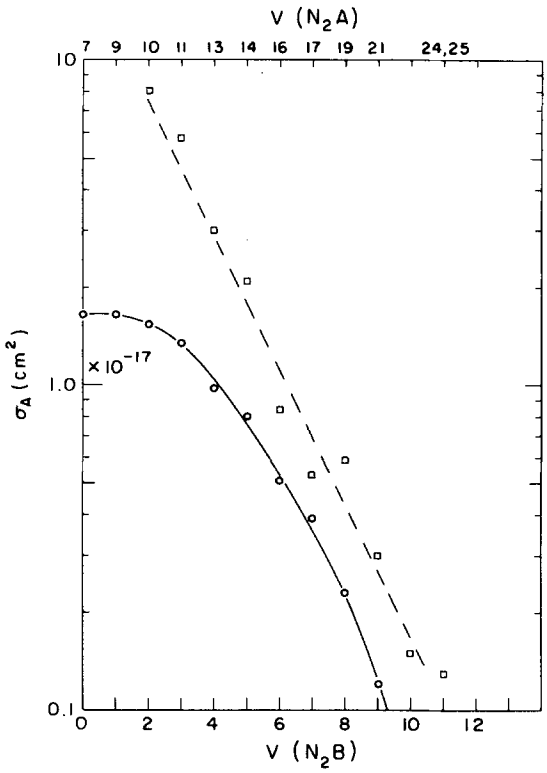

FIG. 10. Electron excitation cross sections ($A\,^3\Sigma_u^+$–$X\,^1\Sigma_g^+$) (see text). □, present estimate. ○, from Ref. 20.

pressure dependent. These two factors are the major source of uncertainty in the estimation of the $\sigma A_v/\sigma B_v$ ratio. The geometric factors have been estimated approximately by calculation of the density distributions for fundamental mode diffusion in a cylinder (Ref. 24), and integration over the field of the spectrometer. The target gas is significantly thick to the electron beam at the higher pressures, introducing uncertainty in relative collection efficiency for the measurement of electron beam current. A rough measure of collection efficiency was made through observations of the N_2^+ 1N(0, 0) band at higher electron energies. However there are obvious uncertainties in extrapolating to lower energies. Estimates of the $\sigma A_v/\sigma B_v$ ratio were therefore made at pressures below 30 mTorr. Although there is good agreement between the calculated [Eq. (10)] and observed curves for the lower N_2B levels (Fig. 3), the higher levels tend to indicate more emission than one would expect at the higher pressures. This may be due to the electron scattering problem or to the observed deviations from linear $[N_2]$ dependence of the $(D2-\bar{d}/\Lambda^2)$ components for the levels in question.

Figure 10 shows the calculated σA_v values based on the Ref. 21a estimates of σB_v. The σA_v numbers are associated with the indicated $A\,^3\Sigma_u^+$ vibrational quantum numbers by assuming that R1 is a resonance process. The reverse process is neglected at the pressures under consideration due to the comparatively high radiative probability of $B\,^3\Pi_g$ molecules. Although the cross sections (σA_v) are determined at the peak energies of σB_v, the numbers should be close to the peaks of the A–X excitation functions, R1′. The Ref. 21a estimates

of σA_v are also shown in the figure. These numbers were determined from electron energy loss spectra[33] assuming a distribution proportional to the $(A-X, v=0)$ Franck–Condon factors. The new values do not conform well with the Franck–Condon distribution and are factors of 1.5–5 larger than the earlier estimates. The total cross section based on the mean of the available numbers in comparison with the mean for a Franck–Condon distribution is $\sum \sigma A_v \approx 3E-16$ cm^2. The deviation of the observed σA_v magnitudes with v from the Franck–Condon shape is not necessarily real. It was necessary to assume in Eq. (10) that $k_1 v = k_3 v$, since $k_1 v$ is not an available quantity. Significant vibrational relaxation or electronic deactivation to a state other than N_2B would introduce inequality of rates and tend to change the estimated σA_v distribution. This would also tend to raise the estimated total cross section. The new σA_v values are the largest reported in the literature. The accuracy of the numbers is difficult to determine due to the uncertainties discussed above. However, we note that the numbers are a minimum estimate due to the assumed equality of R1 and R3, and that if the geometric factors are carried to the extreme, determined by the ratio of the lifetimes of the first and second components, we would have $\sum(\sigma A)_v \approx 2E-16$ cm^2—still a large number. It should be noted that σA_v is determined by the estimated ratio $\sigma A_v/\sigma B_v$ and depends on the σB_v values of Ref. 21a, which have been the subject of controversy and may be regarded as too large in some quarters.[38,39] Values of $\sum \sigma A_v > 3E-16$ cm^2 would be very difficult to cope with in terms of observations of the uv auroral spectrum (cf. Ref. 40) at high altitudes.

The cross section σA_v can also be estimated from the measured values of $I2/I1$ (Eq. (3), Fig. 8). However the results cannot be directly compared with the steady state estimates. The measurements of transient excitation were generally made at energies other than the peak cross section values, and most numbers were obtained near threshold. Furthermore, measurements near the peak cross section tend to result in rather uncertain $I2/I1$ ratios due to the difficulty in separating the weaker $I1$ component at high pressures. The intensity factors in Eq. (3) are generally very sensitive to relatively small errors in the estimation of the damping factors. It can be shown that the measured $I2/I1$ ratios are consistent with the assumed processes.

The ratio $(\sigma B_v/\sigma A_v)$ is related to $I1/I2$ by the relation

$$\sigma B_v/\sigma A_v = k_1 v[N_2](DA_v)^{-1}\left[\left(1-\frac{DA_v}{DB_v}\right)^{-1}\left(\frac{f_1 I1}{f_2 I2}+1\right)-1\right], \quad (11)$$

where

$$DA_v = k_8 + k_3 v[N_2],$$

$$DB_v = AB_v + k_{8'} + k_2 v[N_2],$$

$$f_1 = 1-\exp -DB_v(\Delta t),$$

$$f_2 = 1-\exp -DA_v(\Delta t),$$

and

Δt is excitation pulse width.

Estimation of the cross sections using this method tend to eliminate the electron scattering problem encountered in the steady state observations. Figure 8 shows a calculated curve for the $N_2B\,v=3$ level. At 9.0 eV the estimated $\sigma A_3 = 1.0E-18$ cm^2, and at 13.9 eV $\sigma A_3 = 2.2E-17$ cm^2. The steady state value at the 10.8 eV peak is $\sigma A_3 = 5.8E-17$ cm^2.

The source of the 3rd N_2B decay component is not obvious. At low pressures the damping factor is generally $D3 \simeq 1E4$ sec^{-1} but it is not certain that the lifetime is exactly the same for all levels. At 100 mTorr, $D3 \simeq 1E3$ sec^{-1}. As mentioned in the earlier section one possibility is the energy pooling reaction R10 which has a rate coefficient $k_{10} \approx 3E-10$ cm^{3}sec^{-1} (Ref. 13), since a similar decay is observed in the N_2 2P, $C\,^3\Pi_u - B\,^3\Pi_g$, system (Fig. 9). However the examination of the N_2 2P system is not complete and the pressure dependence has not been established. A rough calculation of diffusion limited energy pooling in the outer volume of the collision chamber suggests that this is only marginally possible as a source. Another possibility is the relaxation of some higher $A\,^3\Sigma_u^+$ state levels not affected by energy resonance with corresponding $B\,^3\Pi_g$ levels. The $B'\,^3\Sigma_u^-$ and $W\,^3\Delta_u$ states are also possible sources, although as noted earlier, there is no sign of the $B'\,^3\Sigma_u^- - B\,^3\Pi_g$ transition in the emission spectrum. The decay of the N_2 2P system also contains three components. The most likely source for the second component appears to be the $E\,^3\Sigma_g^+$ state, which appears to be excited by the Feshbach resonance at 11.48 eV.[41,42] Further investigation is required.

CONCLUSIONS

The N_2 $B\,^3\Pi_g$ state, excited by low energy electrons, is populated by energy transfer processes, even at relatively low pressures. The source appears to be $A\,^3\Sigma_u^+ v > 6$ molecules excited directly by the electrons. The rate coefficients for deactivation of the $A\,^3\Sigma_u^+ v > 6$ levels by $X\,^1\Sigma_g^+$ molecules are large, $8E-12$ cm^2 – $5E-11$ cm^2, and appear to be dominated by electronic deactivation into the $B\,^3\Pi_g$ state. This is presumably due to the close spacing of the potential curves and energies of the two-states. The magnitudes of the rate coefficients suggest that vibrational relaxation of the levels involved in the transfer of electronic energy is not significant. Relaxation of the $A\,^3\Sigma_u^+ v < 7$ levels are less than 10^{-12} cm^3/sec according to Ref. 21b. However a nonlinear dependence on $[N_2]$ observed in some of the higher levels may indicate population by vibrational relaxation; the nonlinearity being due at least partly to an artifact of the analysis system as a result of the combination of two damping factors relatively close together in magnitude. The apparent cross sections for $A\,^3\Sigma_u^+ - X\,^1\Sigma_g^+$ electron excitation are large ($\sum \sigma A_v \approx 3E-16$ cm^2) and do not conform particularly well with the Franck–Condon factor distribution.

The $B\,^3\Pi_g$ state is deactivated by $X\,^1\Sigma_g^+$ at rates which vary between $k_2 v = 1E-11$ cm^{3}sec^{-1} and $1E-10$ cm^{3}sec^{-1}. The distribution of $k_2 v$ is such that the predicted production rates into the $B\,^3\Pi_g$ levels tend to be more uniform in the L–R afterglow than the observed relative emission rates. The results obtained here suggest that

vibrational relaxation in the $B^3\Pi_g$ state is not fast, and probably negligible ($<1E-11$ cm^{3}sec^{-1}) compared to the electronic deactivation rates for most of the levels. The measured radiative transition probabilities of the $B^3\Pi_g$ state agree well with earlier measurements. The distribution of probabilities suggest that the $B^3\Pi_g - W^3\Delta_u$ branch is negligible at any of the observable B levels ($<5\%$) compared to the $B^3\Pi_g - A^3\Sigma_u^+$ radiative probabilities. There is no indication of the $B'^3\Sigma_u^- - B^3\Pi_g$ transition in spectra obtained at pressures up to 100 mTorr.

Although the observations obtained here did not involve reactions with atomic nitrogen, the results are applicable to the L–R afterglow and the aurora. Theories involving the transfer of energy via the $^5\Sigma_g^+$ state as the populating mechanism of at least $B^3\Pi_g$ $v=9-12$ levels require fast vibrational relaxation[2,11,28,29] of the $v=11, 12$ levels. Although the present measurements of $B^3\Pi_g$ deactivation cannot exclude a process of this kind taking place at measureable rates, it does appear unlikely if we accept the present estimates of the relative rates in R2. One would expect a reasonably high transfer probability for the reaction R12 since the process is forbidden only by the $\Delta S=0$ selection rule. Thus it appears that the three body recombination, R7, probably delivers an insignificant amount of energy to the $^5\Sigma_g^+$ state. This conclusion appears to be supported, by the low pressure work of Ref. 6 in which emission rates from N_2B $v=12$ remained below that of N_2B $v=11$ at pressures as low as 30 mTorr where B state deactivation is controlled by radiation. However, other results of this reference are at variance with this paper. Further evidence appears in observations by Ref. 7 in a clean system indicating that the lower levels of the B state decay at a higher rate than N_2B $v=12, 11, 10$ in the late afterglow.

The addition of argon to the afterglow system increases the N_2B emission rate[5,2] and shifts the intensity maximum to lower levels.[2,6,9] The increased intensity is due to a reduced deactivation rate of N_2B, since three body recombination with N_2 replaced by Ar has about the same rate coefficient.[5] However it has been very difficult to explain the N_2B population distribution in terms of a reduction in electronic deactivation and subsequent vibrational relaxation, since the distributions are not linear functions of mole fraction of added gas.[2] It now seems possible this may be explained in terms of the strong dependence of R2 on vibrational level, in combination with some vibrational relaxation in the presence of excess Ar.

Thus according to the evidence obtained here, the production of $B^3\Pi_g$ molecules in the afterglow at all levels is most likely through the $A^3\Sigma_u^+$ state as precursor, by elimination of other possible processes. The present experimental results indicate large rate coefficients for reactions R1 and R3, but can provide no direct evidence that the recombination reaction R5 provides an sufficiently large production rate to explain the observations. Emission from the $A^3\Sigma_u^+$ $v=0, 1$ levels does appear in the L–R afterglow. According to a number of earlier observations[16–19] the $A^3\Sigma_u^+$ $v=0, 1$ molecules are controlled by atomic nitrogen deactivation, R4, with $k_4 \approx 2E-11-5E-11$ cm^{3}sec^{-1}. This would require most of the recombination into the $A^3\Sigma_u^+$ state to ultimately enter the $v=0, 1$ levels. Although we cannot regard the reaction R7 as a resonance processes,[43] the high rate for R1 estimated here would nevertheless deliver most of the energy of R5 into the $B^3\Pi_g$ state. We cannot tolerate a rate for R1 significantly smaller than R3 to provide more energy to the lower $A^3\Sigma_u^+$ levels, since this demands $A^3\Sigma_u^+ - X^1\Sigma_g^+$ electron cross sections too large to be compatible with the high altitude auroral uv spectrum.[40] The compatibility of the present observations with a large rate for R4 thus appears to depend on the rate of the reverse direction of R1. The energy pooling reaction, R9, can also control the A state molecules and according to Ref. 20 this nonlinear factor could produce an apparent dependence on atomic nitrogen with a much smaller k_4 and hence a correspondingly smaller effective rate for $kv_5=0, 1$. The present estimate of R2 implies that only about 25% of the energy of recombination enters the N_2B state. The distribution of the remainder of the energy thus becomes a consideration of some importance.

If we accept the present estimate of the $A^3\Sigma_u^+ - X^1\Sigma_g^+$ electron cross section, the role of the $A^3\Sigma_u^+$ state in the aurora should be reexamined.

ACKNOWLEDGMENTS

This work has been supported by National Science Foundation, Grant # GA-28851, and by the Scaife Foundation.

*Present address: Kitt Peak National Observatory, Tucson, Arizona, 85726. Kitt Peak National Observatory is operated by the Association of Universities for Research in Astronomy, Inc., under contract with the National Science Foundation.

[1]A. N. Wright and C. A. Winkler, *Active Nitrogen* (Academic, New York, 1968).
[2]K. D. Bayes and G. B. Kistiakowsky, J. Chem. Phys. **32**, 992 (1960).
[3]J. F. Noxon, J. Chem. Phys. **36**, 926 (1962).
[4]R. A. Young and R. L. Sharpless, J. Chem. Phys. **39**, 1071 (1963).
[5]I. M. Campbell and B. A. Thrush, Proc. R. Soc. London Ser. A **296**, 201 (1967).
[6]K. H. Becker, E. H. Fink, W. Groth, W. Jud, and D. Kley, Faraday Division of the Chemical Society, Sheffield, April 1972.
[7]A. R. DeMonchy, Ph. D. thesis, University of Minnesota, 1970.
[8]M. A. A. Clyne and D. H. Stedman, J. Phys. Chem. **71**, 3071 (1967).
[9]N. Jonathan and R. Petty, J. Chem. Phys. **50**, 2804 (1969).
[10]F. R. Gilmore, J. Quant. Spectrosc. Radiat. Transfer **5**, 369 (1965).
[11]J. Anketell and R. W. Nicholls, Rep. Prog. Phys. **33**, 269 (1970).
[12]M. Jeunehomme and A. B. F. Duncan, J. Chem. Phys. **41**, 1692 (1964).
[13]E. C. Zipf, Bull. Am. Phys. Soc. **10**, 179 (1965); **13**, 219 (1968).
[14]D. H. Stedman and D. W. Setzer, J. Chem. Phys. **50**, 2256 (1969).
[15]G. N. Hays and H. J. Oskam, J. Chem. Phys. **59**, 6088 (1973).
[16]R. A. Young, Can. J. Chem. **44**, 1171 (1966).

[17]R. A. Young and G. A. St. John, J. Chem. Phys. **48**, 895 (1968).
[18]K. L. Wray, J. Chem. Phys. **44**, 623 (1966).
[19]B. A. Thrush, J. Chem. Phys. **47**, 3691 (1967).
[20]D. E. Shemansky (to be published).
[21](a) D. E. Shemansky and A. L. Broadfoot, J. Quant. Spectroc. Radiat. Transfer **11**, 1401 (1971); (b) J. W. Dreyer and D. Perner, J. Chem. Phys. **58**, 1194 (1973).
[22]D. E. Shemansky and A. L. Broadfoot, J. Quant. Spectroc. Radiat. Transfer **11**, 1385 (1971).
[23]D. E. Shemansky and N. P. Carleton, J. Chem. Phys. **51**, 682 (1969).
[24]J. B. Hasted, *Physics of Atomic Collisions* (Butterworths, Washington, DC, 1964).
[25]E. C. Zipf, J. Chem. Phys. **38**, 2034 (1963).
[26]M. Jeunehomme, J. Chem. Phys. **45**, 1805 (1966).
[27]R. A. Young, G. Black, and T. G. Slanger, J. Chem. Phys. **50**, 303 (1969).
[28]S. W. Benson, J. Chem. Phys. **48**, 1765 (1968).
[29]J. Berkowitz, W. A. Chupka, and G. B. Kistiakansky, J. Chem. Phys. **25**, 457 (1956).
[30]K. A. Saum and W. M. Benesch, Appl. Opt. **9**, 195 (1970).
[31]H. L. Wu and W. Benesch, Phys. Rev. **31**, 172 (1968).
[32]R. T. Brinkmann and S. Trajmar, Ann. Geophys. **26**, 201 (1970).
[33]A. J. Williams and J. P. Doering, Planet. Space Sci. **17**, 1527 (1969).
[34]D. C. Cartwright, Phys. Rev. A **2**, 1331 (1970).
[35]D. E. Shemansky and A. L. Broadfoot, J. Geophys. Res. **78**, 2357 (1973).
[36]D. C. Cartwright, S. Trajmar, and W. Williams, J. Geophys. Res. **76**, 368 (1971).
[37]R. S. Freund, J. Chem. Phys. **51**, 1979 (1959).
[38]W. L. Borst and S. L. Chang, J. Chem. Phys. **59**, 5830 (1973).
[39]D. C. Cartwright, S. Trajmar and W. Williams, J. Geophys. Res. **73**, 2865 (1973).
[40]D. E. Shemansky, E. C. Zipf, and T. M. Donahue, Planet. Space Sci. **19**, 1669 (1971).
[41]J. Comer and F. H. Read, J. Phys. B **4**, 1055 (1971).
[42]R. S. Freund, J. Chem. Phys. **50**, 3734 (1969).
[43]O. Oldenberg, Phys. Rev. **87**, 786 (1952).